IEEE Open Journal of
Power Electronics

Received 25 October 2022; accepted 7 November 2022. Date of publication 14 November 2022;
date of current version 2 December 2022. The review of this article was arranged by Associate Editor Zhixiang Zou.

Digital Object Identifier 10.1109/OJPEL.2022.3222066

Harmonic Voltage Synchronization Using GPS Modules for Grid-Connected Power Converters

LUCAS SAVOI ARAUJO [1], TOMMASO CALDOGNETTO [2] (Senior Member, IEEE), DANILO BRANDAO [1] (Senior Member, IEEE), AND PAOLO MATTAVELLI [2] (Fellow, IEEE)

[1]Grad. Program in Electrical Engineering, Federal University of Minas Gerais, Belo Horizonte 31270-901, Brazil
[2]Department of Management and Engineering, University of Padova, 35122 Vicenza, Italy

CORRESPONDING AUTHOR: TOMMASO CALDOGNETTO (e-mail: tommaso.caldognetto@unipd.it).

This work was supported in part by the Coordenacao de Aperfeicoamento de Pessoal de Nivel Superior - Brasil (CAPES) - Finance Code 001, in part by FAPEMIG, and in part by the Department of Management and Engineering (DTG), Project "ADPE," University of Padova.

ABSTRACT Voltage-controlled inverters (VCI) for distributed energy resources allow operation in grid-connected and islanded conditions. Common techniques based on P-f, Q-V droop-control use sinusoidal voltage references for the VCIs, which brings unwanted circulating harmonic currents in case of connection to grids with distorted voltage. In fact, the voltages at the point of common coupling (PCC) of a sub-grid, like a microgrid, are typically distorted, and the related circulating currents pose potential issues in terms of distribution and converters losses, effectiveness of protections, and power quality. This paper proposes a strategy to synthesize, at the output of a VCI, the same harmonic voltage detected at the PCC to limit unnecessary harmonic current circulation. The proposed method uses global positioning system (GPS) modules to synchronize the harmonic voltage references of the VCIs with the PCC. To this end, low-bandwidth communication is exploited to broadcast the information to distributed VCIs. An experimental setup is implemented to test the proposed control using a hardware-in-the-loop approach for the modeling of the power stage. Several case studies are analyzed, showing the effectiveness of the proposed strategy in achieving power quality improvements: reduced load voltage harmonics, reduced circulating currents, reduced grid current harmonic content, and reduced power losses.

INDEX TERMS Circulating current, distorted voltage, global positioning system, harmonic, synchronization, voltage-controlled inverters.

I. INTRODUCTION

In low-voltage grids, the widespread use of power converters for distributed energy resources (DERs), like photovoltaics and batteries, allows several advantageous functionalities for electrical power systems. However, some challenges still exist toward optimal operation [1]. A relevant power quality issue is the unwanted harmonic current circulation between the converters and the mains when grid voltages are distorted, which is actually a common condition.

Regarding the zero-level control of grid-connected power converters, two main approaches are employed: *i)* current-controlled inverters (CCI) or *ii*) voltage-controlled inverters (VCI). Despite its higher complexity, the VCI approach is prevalent in microgrids (MG), because it allows grid-forming functionality in islanded conditions and smooth transitions between grid-connected and islanded modes [2], [3].

In grid-connected mode, VCIs typically use droop loops (e.g., P-f & Q-V laws) to provide to the inner voltage-control loop a sinusoidal voltage reference that is synchronized with the main grid voltage. Additional outer control loops may also be included to achieve active and reactive output power reference tracking [3], [4]. Notably, the converter voltage references are typically purely sinusoidal.

However, the grid voltage in low-voltage power systems may present significant harmonic components [5]. The IEEE Std. 519-2014 [6], for example, recommends a limit of 8% to the voltage total harmonic distortion (THD) for low-voltage grids. Consequently, when a VCI with purely sinusoidal voltage is connected to a grid with distorted voltage, there is a harmonic current flowing between the two sources due to the different harmonic content. This exchange of harmonic current among the two sources is referred to as *harmonic*

circulation currents herein, analogously to what is done in [7] considering fundamental quantities. Harmonic circulation currents are unnecessary and impair distribution efficiency, effectiveness of protection devices, and further deteriorates the quality of the currents fed at the point-of-common-coupling (PCC) of the MG.

The distortion of low-voltage grids is usually due to voltage drops along line impedances caused by non-linear loads or non-linear effects of medium-voltage to low-voltage transformers. Thus, some works propose to use power converters to compensate the related harmonic currents directly [8], [9], [10]. In this approach, the non-linear load current, or the grid current, is sensed and used to generate the current compensation reference. Regarding harmonic voltage compensation, the converter control commonly uses the PCC voltage and a virtual impedance in the control loop to generate a voltage reference for compensating the distortion [11], [12], [13]. The main drawback of these approaches is that measuring the PCC voltage or current as quantities used directly in the control is not practical, due to the distance of the MG PCC from the distributed converters. Also, the performance of this type of strategy often depends on the specific values of the line impedances. Some works contemplate approximating the PCC voltage with the voltage at the point-of-connection (POC) [14], but this is not always acceptable, due to the differences in voltage amplitude and phase related to the circulation of fundamental active and reactive power through the distribution lines. Notably, this issue is particularly relevant for the reduction of harmonic circulation currents aimed herein. The PCC/POC approximation for harmonic circulation current reduction is used in [15], where, instead of measuring the PCC voltage and using it directly in the control loop, low-bandwidth communication is applied for sending PCC voltage harmonic amplitude to the converters. The PCC voltage harmonic components are extracted in a synchronous reference frame and then transmitted to each converter controller, then the transmitted data consists of mainly dc signals. In this approach, the angle used in the Park transformations performed in the converter control and in the PCC measurement block may differ, due to phase-shifts related to power circulation along the distribution lines and the fact that the two systems are not synchronized. This impairs the quality of the performed compensation.

Recently, the use of global positioning system (GPS) technology has attracted interest as one of the several options to achieve the synchronization of converters in low-voltage MGs. In [16], the GPS signal is used to directly synchronize the microprocessors clock of droop-based grid-forming inverters in order to maintain the parallelism of the converters. In [17] and [18], the GPS is used together with advanced phase-locked-loops (PLLs) to improve the synchronization of dispersed converters and the main grid. These proposals rely on communication, being the rotating angle of the grid voltage transmitted to the converters.

GPS synchronization is also employed in converters control to perform harmonic current sharing between the converters [19] or to overcome frequency and phase deviations during the islanded operation of an MG [20], [21], [22], [23]. Thus, the converters may operate as isochronous generators, keeping the frequency fixed [24]. However, these approaches are applied only to islanded MGs and do not consider the grid-connected mode. Furthermore, control validation by real GPS modules is not always performed. In summary, the use of synchronization means like GPS signals to improve the performance of grid-connected power converters connected to low-voltage grids is currently relatively new and only partially explored in the literature.

The main contribution of this paper is the proposal of a novel strategy to synthesize, at the output of the VCIs, the same harmonic voltage detected at the PCC. The harmonic voltage reference for the VCIs is synchronized with the PCC harmonic voltage using GPS modules, and its phase synchronization information and amplitude are broadcast by low-bandwidth communication. The proposed approach targets grid-connected MGs in which VCIs are distributed over the grid and may be located relatively far from each other and the PCC. Thus, dedicated high-performance communication for achieving synchronization may not be easily available. The paper extends the preliminary results originally presented in [25], by reporting herein additional analyses and implementation details, extended literature review, experimental validations, and results discussion.

The proposed control is developed in a hardware-in-the-loop experimental setup. It is compared with conventional droop-control with an outer power loop and with the harmonic rejection approach. The results show that the proposed control is the most effective in compensating for the harmonics of the grid current. Thus, the load-voltage is indirectly improved, and the circulating current and the power losses are reduced. The proposed synchronization strategy can be potentially applied to enhancing other existing control functions, like, for example, the one in [8] related to the sharing of harmonic currents between distributed converters.

II. PRINCIPLES OF CONVERTERS SYNCHRONIZATION

The proposed control aims to synthesize at the output capacitor of a VCI the same harmonic voltages detected at the PCC of the grid subsection to which it is connected. To this end, the harmonic components to be compensated must have the same amplitude and phase, that is, they must be synchronized. However, the PCC may be physically distant from the converter, as shown in typical environments, like, for example, in [26]. This makes it challenging to measure the PCC voltage in real-time and use it directly in a VCI control loop.

A solution to achieve the desired features using existing low-bandwidth communication consists in communicating only dc variables between the control agents. This section gives the theoretical background for representing a time-varying phasor using dc variables that can be communicated

to a different location and then allow a subsequent reconstruction of the original signal.

A. THEORETICAL BACKGROUND

Consider the h-th harmonic component $v_h = V_h \sin(h\omega t)$ superimposed to a distorted grid voltage, where V_h is the amplitude of the harmonic and ω is the fundamental grid-voltage frequency. Consider two unitary orthogonal signals, $v_{\parallel,h} = \cos(h\omega t + \phi_h)$ and $v_{\perp,h} = \sin(h\omega t + \phi_h)$, at the same harmonic component frequency. Be ϕ_h the phase-difference between the harmonic and the orthogonal voltages.

By multiplying the harmonic component by twice the voltage $v_{\perp,h}$, it yields:

$$\begin{aligned}\widetilde{v}_{qh} &= 2 \cdot v_h \cdot v_{\perp,h} = 2 \cdot V_h \sin(h\omega t) \cdot \sin(h\omega t + \phi_h) \\ &= V_h \left[\cos\phi_h - \cos\left(2\, h\omega t + \phi_h\right)\right] , \end{aligned} \tag{1}$$

where the former component is constant and related to the amplitude of the h-th harmonic projected along $v_{\perp,h}$, the latter is an oscillatory component at frequency $2h\omega$. Then, the dc component, which can be estimated by appropriate low-pass filtering, is:

$$v_{qh} = V_h \cos\phi_h \, . \tag{2}$$

The same procedure considering the signal $v_{\parallel,h}$ gives:

$$\begin{aligned}\widetilde{v}_{dh} &= 2 \cdot v_h \cdot v_{\parallel,h} = 2 \cdot V_h \sin(h\omega t) \cdot \cos(h\omega t + \phi_h) \\ &= V_h \left[-\sin\phi_h + \sin\left(2\, h\omega t + \phi_h\right)\right] \end{aligned} \tag{3}$$

$$v_{dh} = \; -V_h \sin\phi_h \tag{4}$$

Then, the dc terms v_{dh} and v_{qh} can be communicated to other remote converters and allow to reconstruct a replica v_h^* of the original signal v_h, if the base $v_{\perp,h}$, $v_{\parallel,h}$ is known, as:

$$\begin{aligned} v_h^* &= v_{qh} \cdot \sin(h\omega t + \phi_h) + v_{dh} \cdot \cos(h\omega t + \phi_h) \\ &= V_h \cos\phi_h \, \sin(h\omega t + \phi_h) - V_h \sin\phi_h \, \cos(h\omega t + \phi_h) \\ &= V_h \sin(h\omega t) \end{aligned} \tag{5}$$

Notably, the reconstructed harmonic voltage in (5) is virtually identical to the original signal v_h, thus, it can be used as a reference to synthesize that harmonic voltage at the converter output.

Of course, the signals $v_{\perp,h}$, $v_{\parallel,h}$ should be uniquely and autonomously determined by both the sender and the receiver of the terms (2) and (4). To this end, different approaches may be adopted. The use of GPS synchronization means is proposed and explored herein.

B. PHASE-MISMATCH INFLUENCE IN PARALLEL VOLTAGE-SOURCES

The connection of a VCI to an electric grid can be simplified as two voltage-sources connected by a series impedance as shown in Fig. 1, where V_{ch} is the converter h-th harmonic voltage amplitude, V_{gh} is the grid h-th harmonic voltage amplitude, θ_h is the phase-difference between the harmonic voltages, j is the imaginary unit, and R and L are the

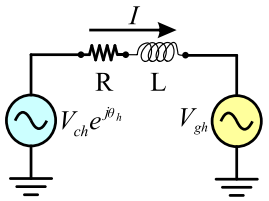

FIGURE. 1. Simplified model of a grid-connected converter.

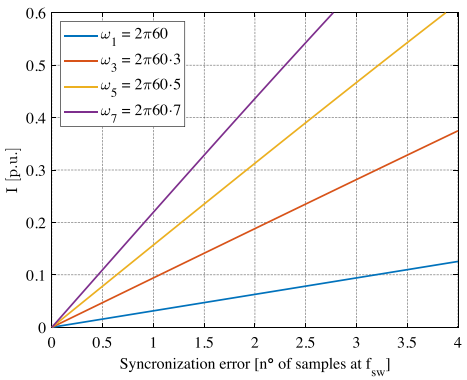

FIGURE. 2. Normalized relations between synchronization error and current flow.

impedance resistance and inductance, respectively. The harmonic circulation current between the two sources can be computed as:

$$I = \frac{V_{ch}e^{j\theta_h} - V_{gh}}{R + j\omega_h L} \tag{6}$$

Assuming equal amplitudes for the harmonics, that is, $V_{ch} = V_{gh}$, and $\theta_h = \omega_h t$, (6) can be rewritten as:

$$I = \frac{V_{ch}(e^{j\omega_h t} - 1)}{R + j\omega_h L} \, , \tag{7}$$

which is represented in Fig. 2 normalized by the term:

$$I_0 = \frac{V_{ch}}{R + j\omega_h L} \tag{8}$$

Fig. 2 shows the influence of the synchronization accuracy with respect to the harmonic current suppression. The current amplitude is reported in *p.u.* and the synchronization error in terms of number of samples, considering a sampling frequency of 12 kHz. Notably, if both the voltages are perfectly synchronized there is no current flow between the sources. However, a small error (e.g., two samples) is sufficient to cause a considerable current flow depending on the grid parameters (8). Moreover, higher-order harmonics are more sensitive to synchronization accuracy. These kinds of considerations are important in order to design the accuracy of the synchronization equipment (e.g., GPS module) or the sampling frequency of the controller, in relation to the targeted impact on current suppression.

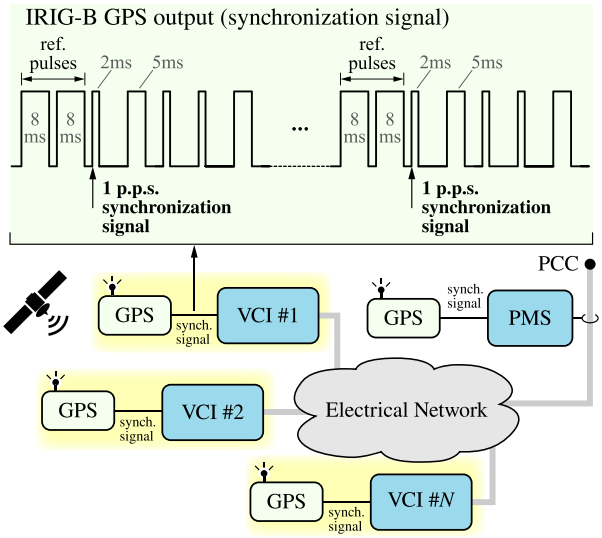

FIGURE. 3. Synchronization of units using GPS modules.

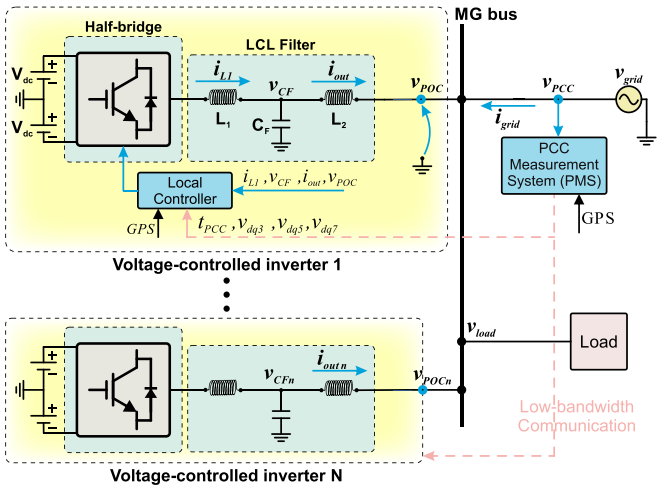

FIGURE. 4. Application example of the proposed control.

C. SYNCHRONIZATION BY GPS MODULES

The GPS is a widely used satellite-based radio-navigation system that provides geographic position to a receiver as well as accurate time information. GPS receiver modules typically convey timing information by a digital output signal using the IRIG-B timecode [27]. Such signals at the output of the GPS modules, which may be located at different sites, are all synchronized (typ., ±100 ns accuracy). Therefore, the GPS IRIG-B signals are often employed for transferring timing information or to derive trigger signals for synchronized measurement, automation, or control functions. A sample of an IRIG-B signal is displayed in Fig. 3. Two consecutive pulses lasting 8 ms, referred to as *Ref.*, occur once per second and indicate the beginning of a new 1-s time frame. Herein, only the rising edge of the first pulse after *Ref.* is used as a 1-pulse-per-second (p.p.s.) synchronization signal. For the sake of completeness, the additional pulses within the 1-s time frame that separate consecutive *Ref.* pulses in the IRIG-B timecode can be decoded to retrieve information, for example, on the second, minute, hour, and day synchronized to UTC of a specific time instant [27].

The main purpose of the GPS in this work is to obtain a common synchronization signal to all the compensation players, that is, to the VCIs and the PCC measurement system (PMS), which are introduced in the next Section III. The considered synchronization signal herein is the couple of *Ref.* pulses, highlighted in Fig. 3, which are synchronized at each VCI and the PMS thanks to the GPS modules. Of course, other synchronization techniques may be adopted (see, e.g., [28]) to implement the technique proposed in this manuscript to limit unnecessary harmonic circulation currents. The GPS approach has been adopted herein for its simple implementation and its common use in power systems automation and measurements, like in phasor measurement units (PMUs) [29].

III. GPS-BASED HARMONIC VOLTAGE SYNCHRONIZATION

The proposed strategy is performed by two main players, visible in Fig. 3, that are equipped with GPS modules:

- PMS, which estimates the parameters (i.e., amplitude and phase) of the main grid voltage, and
- VCIs distributed within the considered sub-grid, like, an MG.

An application example of the proposed control is shown in Fig. 4 .

The PMS is responsible for detecting the harmonic components of the PCC voltage v_{dqh} and for calculating the time interval t_{PCC} between the GPS signal and the first positive zero crossing of the PCC voltage. The quantities are then sent to the distributed VCI by low-bandwidth communication. Details of the PMS are described in Section III-A.

The local controllers of the VCIs receive the quantities sent by the PMS and, based on their local GPS signals, they generate a harmonic voltage reference of the same amplitude and phase as the corresponding harmonic voltage at the PCC. The fundamental voltage reference is provided to a droop-based controller. The VCI control is discussed in more detail in Section III-B.

A. PCC MEASUREMENT SYSTEM (PMS)

The scheme of the PMS is displayed in Fig. 5a. Two main tasks are performed in the PMS: *i)* calculate the amplitude (i.e., v_{dh} and v_{qh}) of the PCC harmonic voltages of interest; and *ii)* calculate the time interval t_{PCC} between the GPS signal and the PCC voltage at zero crossing, required for synchronization.

The amplitude of each h-th harmonic component (e.g., $h = 3, 5, 7$) is calculated in the so-called "Harmonic Detection block," shown in Fig. 5c. It is necessary to implement one harmonic detection block for each harmonic component to be compensated. To this end, the fundamental component of the

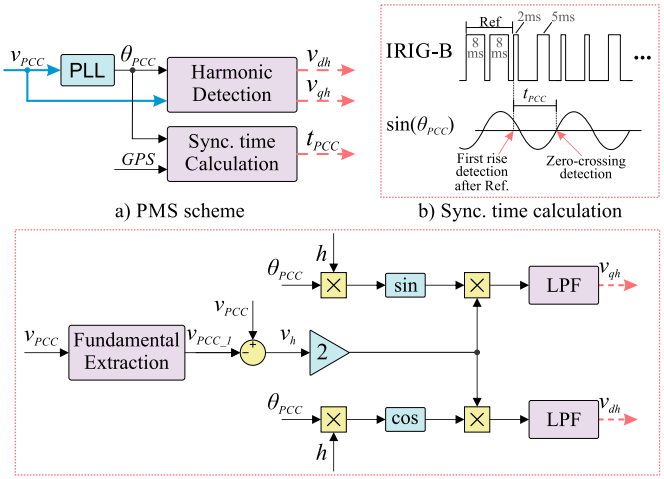

FIGURE. 5. PCC Measurement System structure.

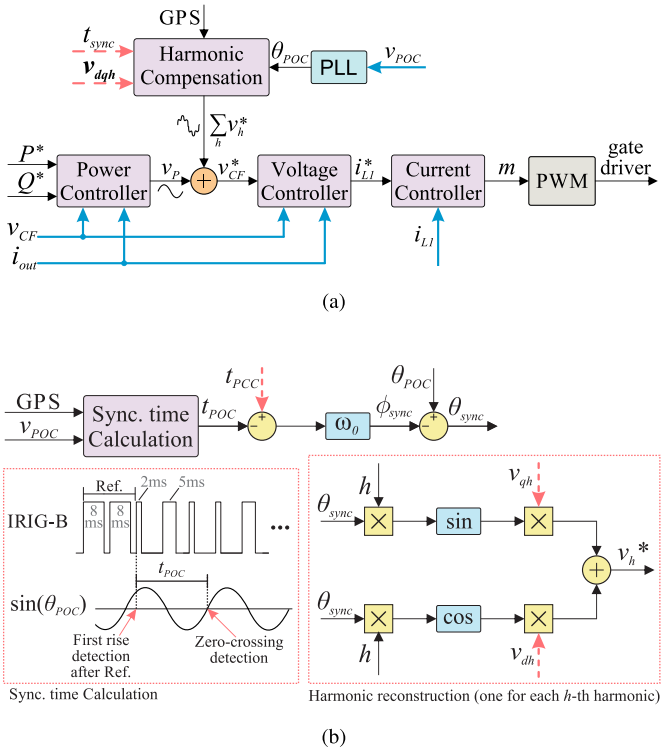

FIGURE. 6. a) VCI control structure; b) Harmonic compensation block detailed.

total PCC voltage, indicated as v_{PCC_1}, is firstly obtained and subtracted from the PCC voltage, in order to consider only the harmonic content. Two orthogonal voltages at the specific h-th harmonic component (i.e., $v_{\perp,h}$ and $v_{\parallel,h}$, defined in Section II) are then created and multiplied by the PCC harmonic components. After processing the result through a low-pass filter (LPF) to extract the dc value of interest, the amplitude of the direct (i.e., v_{dh}) and quadrature (i.e., v_{qh}) components are obtained and broadcast to the distributed VCIs. In this implementation, a discrete second-order LPF with a cut-off frequency of 8 Hz and a damping ratio of 0.707 is used. The PCC voltage angle θ_{PCC} is obtained through a PLL, specifically, the one presented in [30], which, by a proper design of the loop bandwidth (e.g., 3 Hz in the following validation, in Section IV), allows to estimate the grid angle θ_{PCC} with negligible effects from the harmonics that are present in the grid voltage.

The time interval t_{PCC} between the GPS synchronization signal and the PCC voltage at zero crossing is also calculated, as shown in Fig. 5b. This information is broadcast to the VCIs and used for the synchronization of the harmonic components.

B. VOLTAGE-CONTROLLED INVERTER CONTROL

The control scheme at the VCI side is shown in Fig. 6a. The control is composed of three cascaded loops, that is, power, voltage, and current, that generate the PWM pulses to the gate driver of the converter. The outer power controller is based on the well-known droop control to define the fundamental component of the voltage reference v^*_{CF}. To allow active and reactive output power tracking, an integrative regulator is adopted in the power controller as described in [2] and [3]. The voltage controller uses ordinary proportional-resonant regulators for each harmonic that should be compensated, while the current controller uses a proportional regulator.

The voltage reference for the h-th harmonic v^*_h is defined by the "Harmonic Compensation" block, detailed in Fig. 6b.

First, the GPS signal is used to calculate the time delay t_{POC} between the zero-crossing of the POC fundamental voltage v_{POC_1} and the first rising edge after *Ref.* pulses from the local GPS signal, analogously to what is described in Section III-A for the PMS. Based on the received t_{PCC} broadcast by the PMS, and the local measurements t_{POC} and θ_{POC}, a synchronized phase θ_{sync} that estimates the phase of the PCC voltage θ_{PCC} can be computed as shown in Fig. 6b:

$$\begin{aligned}\theta_{sync}(t) &= \theta_{POC}(t) - \phi_{sync}(t) \\ &= \underbrace{\omega_0 t - \omega_0 t_{POC}}_{\theta_{POC}(t)} - \underbrace{\omega_0 \left(t_{PCC} - t_{POC}\right)}_{\phi_{sync}} \\ &= \omega_0 t - \omega_0 t_{PCC} = \theta_{PCC}(t)\end{aligned} \tag{9}$$

that is used for harmonic synchronization, where t represents physical time. Thereby, based on the harmonic amplitudes v_{qh} and v_{dh} transmitted by the PMS, it is possible to rebuild the harmonic voltage v^*_h that was detected at the PCC. The harmonic reconstruction involves all the harmonics to be compensated. The references of each h-th harmonic v^*_h are summed together in the term $\sum_h v^*_h$ and added to the VCI voltage controller reference, as shown in Fig. 6a, to reproduce at its output terminals virtually the same harmonic content of the PCC voltage.

IV. EXPERIMENTAL RESULTS

Fig. 7 shows the hardware-in-the-loop (HIL) experimental setup used to validate the proposed control. The electrical

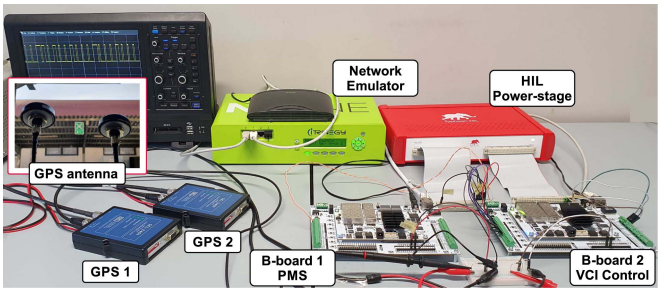

FIGURE. 7. Experimental setup for the proposal validation.

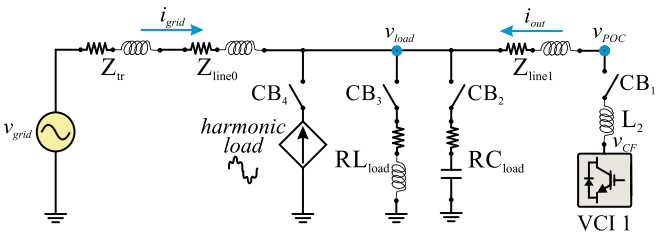

FIGURE. 8. Electrical circuit implemented in HIL.

circuit of Fig. 8, representing the power stage, is implemented in Typhoon HIL. The scenario consists of a VCI connecting a DER to the main grid with different loading conditions considered to evaluate the proposal operation, including RL load, RC load, and non-linear load. The PMS and the VCI control are deployed in two different Imperix B-Board controllers, which generate the PWM control signals based on the measured currents and voltages of the converter emulated in the HIL system. The PMS communicates the control quantities to the VCI by Ethernet UDP protocol. The communication line is processed through a dedicated network emulator by iTrinegy NE-ONE to emulate realistic conditions in terms of, for example, bandwidth, congestion, latencies, and packet loss. Each B-Board controller is connected to an independent SEL-2401 GPS module, which provides the IRIG-B output with $\pm$ 100 ns timing accuracy. The results are evaluated considering three VCI control approaches:

1) Conventional control of the VCI, without harmonic compensation, that is, $\sum_h v_h^*$ is set to zero;
2) Harmonic rejection in the converter output current, that is, $\sum_h v_h^*$ is defined based on v_{POC} measurement instead of v_{PCC}, so the converter synthesizes a voltage v_{CF} with harmonics equal to those of v_{POC} in Fig. 4 avoiding any harmonic circulation currents at the output;
3) Harmonic compensation proposed in this paper, with $\sum_h v_h^*$ defined as in Fig. 6.

Four different case studies are considered to verify the effectiveness of the proposed control. The first three cases consider distorted grid voltage with linear loads, while the last case considers a pure sinusoidal grid-voltage with a non-linear load. System parameters, including line impedance values and grid voltage harmonic content, are listed in Table 1. In the following, operation with distorted grid voltage indicates that the 3-rd, 5-th, and 7-th harmonics, as specified in Table 1, are simultaneously present. The considered parameters are typical for low-voltage distribution networks (see, e.g., [26]).

TABLE 1. System Parameters

Parameter	Value	Parameter	Value
Grid frequency (ω_0)	$2\pi 60$ rad/s	VCI power (Sn)	8.48 kVA
Grid voltage (V_0)	$127\sqrt{2}$ V	Inductor L_1	4.5 mH
3-rd harmonic	$5\%V_0\angle 15\,^\circ$	Capacitor C_F	140 μF
5-th harmonic	$4.5\%V_0\angle 25\,^\circ$	Inductor L_2	62.5 μH
7-th harmonic	$4\%V_0\angle 35\,^\circ$	Switching frequency	24 kHz
Grid voltage THD	7.83 %	R_{RC} load	0.19 Ω
Z_{tr}	$(9.5\text{m} + j\omega 62.5\mu)\ \Omega$	C_{RC} load	15.3 mF
Z_{line0}	$(30\text{m} + j\omega 10\mu)\ \Omega$	R_{RL} load	0.33 Ω
Z_{line1}	$(30\text{m} + j\omega 10\mu)\ \Omega$	L_{RL} load	0.89 mH

A. DISTORTED GRID VOLTAGE–NO LOAD

The situation with VCI connected to a distorted grid voltage but without any load connected (i.e., CB_2-CB_4 in Fig. 8 open) is considered first. The grid voltage and current waveforms are shown in Fig. 9. When the conventional control is employed, the VCI output voltage is kept sinusoidal, which produces a noticeable circulating current between the grid and the converter, as shown in Fig. 9a. Such current can cause converter control saturation, protection tripping, and/or operation interruptions. The issue is overcome by the proposed harmonic compensation strategy.

When the proposed harmonic compensation is employed, the VCI voltage presents the same harmonic content as the grid voltage measured at the PCC, as shown in Fig. 9c. Thus, the grid circulating current is drastically reduced from 89 A to 1.05 A, and the line impedance losses decreased from 118 W to 0.08 W. In this scenario (i.e., no load), there is no phase-shift between the PCC and POC voltages, then the implementation of harmonic rejection performs similarly to harmonic compensation, as visible comparing Figs. 9b and 9c.

B. DISTORTED GRID VOLTAGE–RC LOAD

The second case study considers the RC load in Fig. 8 connected (i.e., CB_2 closed). In this way, the situation in which the POC voltage is phase-shifted from the PCC voltage is evaluated. The POC fundamental voltage is 10° lagged from the PCC voltage. Other network configurations with different load and generation conditions could cause similar effects. The results are shown in Fig. 10.

The grid current without the VCI (i.e., CB_1 open) shows a THD value of 9%. When conventional control is active, a high harmonic current flows from the VCI to the grid; this situation increases further the grid current THD, which rises to 10.2%. The harmonic rejection strategy synthesizes the same

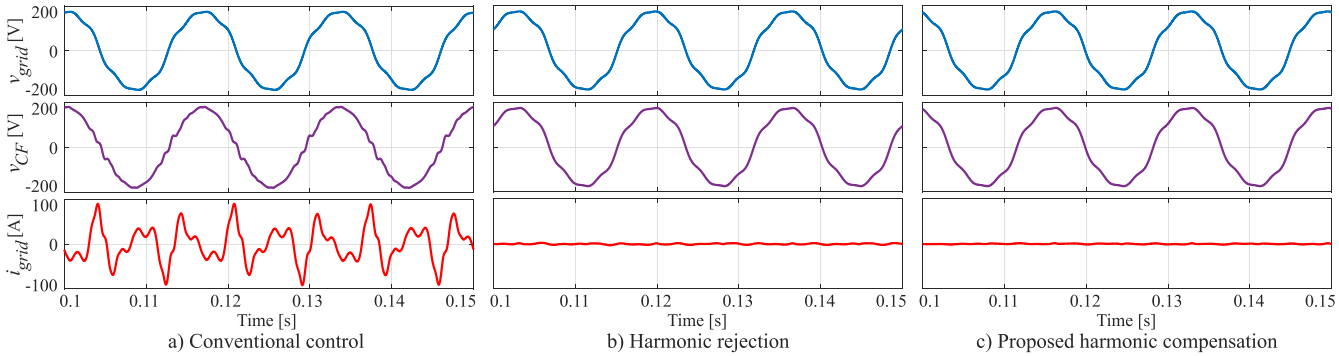

FIGURE. 9. Distorted grid voltage with no load. b) and c) are capable of limiting circulating harmonics in the grid current.

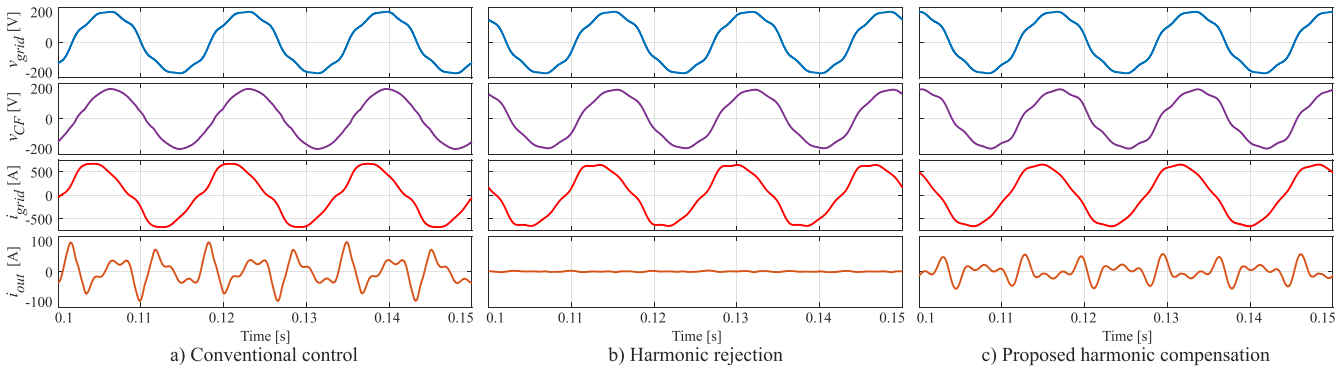

FIGURE. 10. Distorted grid voltage with RC load. The proposed approach in c) harmonic circulation currents due to grid-voltage distortions and contributes to supplying the local load. The grid current THD is equal to 10.2%, 9.1%, and 5.7% in a), b), and c), respectively.

harmonic voltage of the POC voltage and, thus, successfully inhibits the VCI harmonic current flow. But, the grid current THD only slightly reduces to 9.1%.

The proposed harmonic compensation, instead, synthesizes the same PCC voltage in the converter output capacitor, which causes a harmonic current flow that contributes to the load harmonic current. Thus, the VCI current presents a higher harmonic content than the harmonic rejection approach. However, this is a better condition for the system overall operation because it reduces the losses in the line impedances and the grid current harmonics. In this case, grid current THD improves to 5.7%. Besides, by compensating for the mains current, the quality of the local voltage also improves.

Remarkably, this case study also shows that the use of the POC voltage instead of PCC voltage as an approximation for voltage compensation [14] could result in inappropriate compensation due to the phase-shift between the two.

C. DISTORTED GRID VOLTAGE–RL LOAD

This section considers the RL load in Fig. 8 connected (i.e., CB_3 closed). When the VCI is disconnected, the grid-voltage harmonics result in a correspondingly distorted load current, with a THD value of 2.5%. In this case study, the VCI is set to provide active and reactive power of 6 kW and 6 kVAr, respectively. Fig. 11a displays the obtained results by using a conventional control for the VCI, in which a pure sinusoidal voltage is given as a reference to the converter voltage controller, as commonly done in classical droop control. In this case, the grid current shows a THD of 22.4%. Using the harmonic rejection approach, a substantial improvement is noted in the VCI current (THD of 2.3%) but, on the other hand, a worse grid current (THD of 3.7%) than the situation without VCI, as shown in Fig. 11b.

The proposed harmonic compensation is implemented with a poor quality communication of bandwidth of 0.512 Mbps, a latency of 35-60 ms, and a 5% of packet loss. The results are shown in Fig. 11c, in which a better grid current shape is noted (THD of 1.9%), due to the VCI harmonics contribution (THD of 5.7%). It can be noticed that the proposed approach does not interfere with the active and reactive power supply of the converter, and poor quality communication does not affect the operation performance.

D. SINUSOIDAL GRID VOLTAGE–DISTORTED LOAD

This last case study considers the grid voltage as purely sinusoidal and a controlled current source as a load. The current source is set to drain only harmonic current ($h = 3, 5, 7$), so that the voltage drop in the line impedance causes a distorted voltage at the point of connection of the load, with a voltage THD value of 6.5%. With the VCI switched off (i.e.,

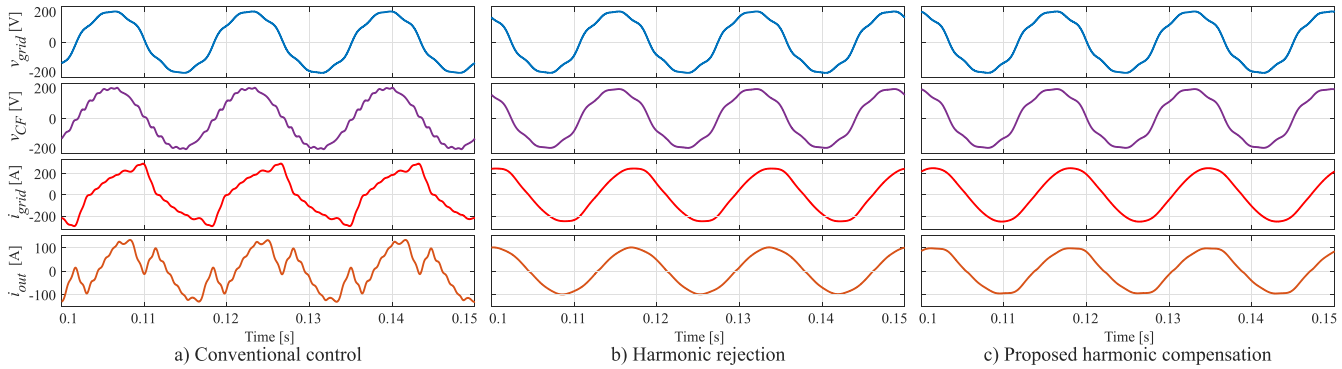

FIGURE. 11. **Distorted grid voltage with RL load. The proposed approach in c) limits harmonic circulation currents due to grid-voltage distortions and contributes to supplying the harmonics absorbed by the local load. The grid current THD is equal to 22.4%, 3.7%, and 1.79% in a), b), and c), respectively.**

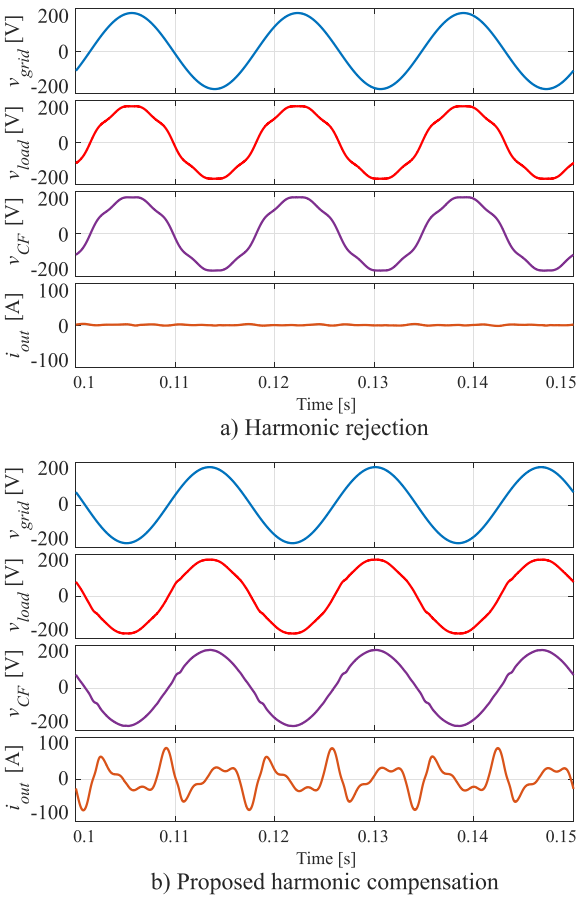

FIGURE. 12. **Sinusoidal grid voltage with distorted load. The proposed approach improves load voltage THD, which equals 6.5% in a) and 3.5% in b).**

CB_1 open), the total losses in the line impedance amount to 1683 W.

Fig. 12a shows the behavior of the system using the harmonic rejection approach. The output voltage of the VCI has a similar shape to the load voltage. Thus, the VCI does not provide current to the grid, and the load voltage THD is kept at 6.5%. Using the proposed harmonic compensation, the VCI synthesizes a pure sinusoidal voltage, as it is the one at the PCC, as shown in Fig. 12b. Hence, the VCI automatically shares the load harmonic current, reducing the voltage drop across the line impedances, and improving the load voltage quality (THD of 3.5%). Moreover, the total line impedance losses are reduced to 1600 W.

In this case, the waveforms under conventional control are not included: these would be identical to those of the proposed compensation method. In fact, in this test the grid voltage is purely sinusoidal, which means that $\sum_h v_h^*$ is equal to zero, as in the case of conventional control according to the definition at the beginning of this Section IV. It may be worth emphasizing that what is reported in Fig. 12 highlights one of the merits of the proposed approach over the harmonic rejection method: the proposed approach supports the grid voltage, helping, as a consequence, to improve the local load voltage THD (note, 3.5% by the proposed approach, 6.5% by the harmonic rejection method). In fact, the harmonic rejection control implements an equivalent high impedance at the harmonics, which impedes the VCI from generating the harmonic currents requested by the nonlinear load. Therefore, it does not support the grid in feeding the nonlinear load, which results in a higher load voltage THD. This drawback of the harmonic rejection control is not present with the conventional control, which, on the other hand, suffers from the issue tackled in the manuscript, that is, it suffers from undesired harmonic circulation currents when the grid voltage is distorted.

E. SUMMARY OF RESULTS

Table 2 shows a performance comparison of the considered four case studies regarding line impedance power losses, THD values of the grid and VCI currents, and THD values of the load voltage. In general, the conventional approach is the worst, as expected. Instead, the harmonic rejection approach is the best regarding the converter stress, as it presents the lowest THD for the VCI current. Finally, the proposed harmonic compensation strategy improves the power quality of the grid current and of the load voltage, as remarked at the end of Section IV-D, and also presents the lowest overall line power losses.

TABLE 2. Summary of Approaches Performances

Case study	no-load	RC-load	RL-load		nonlinear-load	
Control adopted	Losses	THD i_{grid}	THD i_{grid}	THD i_{out}	Losses	THD v_{load}
Conventional control	118 W	10.2%	22.4%	55.5%	1600 W	3.5%
Harmonic rejection	0.1 W	9.1%	3.7%	2.3%	1683 W	6.5%
Harmonic compensation	0.08 W	5.7%	1.9%	5.7%	1600 W	3.5%

Based on the presented results, the proposed harmonic compensation shows the best efficiency and power quality. This solution can be implemented in distributed VCIs installed in an MG without needing high-performance communication means.

V. CONCLUSION

This paper addressed the harmonic circulating current issue caused when a voltage-controlled inverter with a pure sinusoidal voltage output is connected to a grid with distorted voltage. To overcome this problem, a harmonic voltage compensation strategy is proposed, in which the voltage-controlled inverter synthesizes the same harmonic voltage detected at the PCC. Global positioning system (GPS) modules are exploited to perform the needed synchronization between the PCC and the voltage-controlled inverter harmonics. An experimental setup using hardware-in-the-loop with external controllers, together with commercial GPS modules, and a communication network emulator, was used to test the proposed approach. The proposal was compared with two other approaches: 1) the classical droop control with an external power loop and 2) the harmonic rejection approach. Four case studies were considered to verify the control performance in different system conditions. The proposed harmonic compensation performs the best reduction in the grid current THD, indirectly improving load voltage and reducing line power losses. However, the reproduction of the harmonics by the converter may potentially increase its losses in some conditions, which is an aspect that dedicated studies may address. The reported results show that increasing the converter output impedance, as obtained by the harmonic rejection control, impedes the converter from generating output harmonic currents and, therefore, from supporting the grid in feeding harmonic currents absorbed by nonlinear loads that may be connected locally. This brings to a worse voltage quality than in the case of the proposed control. This drawback of the harmonic rejection control is not present with the conventional control based on the classical droop control, which, on the other hand, suffers from the issue tackled in the manuscript, that is, it suffers from undesired harmonic circulation currents when the grid voltage is distorted.

REFERENCES

[1] T. Ackermann and V. Knyazkin, "Interaction between distributed generation and the distribution network: Operation aspects," in *Proc. IEEE/PES Transmiss. Distrib. Conf. Exhib.*, 2002, pp. 1357–1362.

[2] S. Lissandron and P. Mattavelli, "A controller for the smooth transition from grid-connected to autonomous operation mode," in *Proc. IEEE Energy Convers. Congr. Expo.*, 2014, pp. 4298–4305.

[3] L. S. Araujo and D. I. Brandao, "Self-adaptive control for grid-forming converter with smooth transition between microgrid operating modes," *Int. J. Elect. Power Energy Syst.*, vol. 135, 2022, Art. no. 107479.

[4] T. Caldognetto, H. Abedini, and P. Mattavelli, "A per-phase power controller for smooth transitions to islanded operation," *IEEE Open J. Power Electron.*, vol. 2, pp. 636–646, 2021.

[5] J. Lundquist, "On harmonic distortion in power systems," M.S. thesis, Dept. Electric Power Eng., Chalmeers Univ. Technology, Gothenburg, Sweden, 2001.

[6] *IEEE recommended practice and requirements for harmonic control in electric power systems*, IEEE Std. 519-2014 (Revision of IEEE Std. 519-1992), 2014.

[7] P. Tenti, A. Costabeber, P. Mattavelli, and D. Trombetti, "Distribution loss minimization by token ring control of power electronic interfaces in residential microgrids," *IEEE Trans. Ind. Electron.*, vol. 59, no. 10, pp. 3817–3826, Oct. 2012.

[8] A. M. dos Santos Alonso, D. I. Brandao, T. Caldognetto, F. P. Marafão, and P. Mattavelli, "A selective harmonic compensation and power control approach exploiting distributed electronic converters in microgrids," *Int. J. Elect. Power Energy Syst.*, vol. 115, 2020, Art. no. 105452.

[9] J. He and Y. W. Li, "Hybrid voltage and current control approach for DG-grid interfacing converters with LCL filters," *IEEE Trans. Ind. Electron.*, vol. 60, no. 5, pp. 1797–1809, May 2013.

[10] J. He, Y. W. Li, and F. Blaabjerg, "Flexible microgrid power quality enhancement using adaptive hybrid voltage and current controller," *IEEE Trans. Ind. Electron.*, vol. 61, no. 6, pp. 2784–2794, Jun. 2014.

[11] J. He, Y. W. Li, and M. S. Munir, "A flexible harmonic control approach through voltage-controlled DG-Grid interfacing converters," *IEEE Trans. Ind. Electron.*, vol. 59, no. 1, pp. 444–455, Jan. 2012.

[12] X. Zhao, L. Meng, C. Xie, J. M. Guerrero, and X. Wu, "A unified voltage harmonic control strategy for coordinated compensation with VCM and CCM converters," *IEEE Trans. Power Electron.*, vol. 33, no. 8, pp. 7132–7147, Aug. 2018.

[13] R. A. Mastromauro, M. Liserre, T. Kerekes, and A. Dell'Aquila, "A single-phase voltage-controlled grid-connected photovoltaic system with power quality conditioner functionality," *IEEE Trans. Ind. Electron.*, vol. 56, no. 11, pp. 4436–4444, Nov. 2009.

[14] Y. W. Li and J. He, "Distribution system harmonic compensation methods: An overview of DG-interfacing inverters," *IEEE Ind. Electron. Mag.*, vol. 8, no. 4, pp. 18–31, Dec. 2014.

[15] M. Savaghebi, J. C. Vasquez, A. Jalilian, J. M. Guerrero, and T.-L. Lee, "Selective compensation of voltage harmonics in grid-connected microgrids," *Math. Comput. Simul.*, vol. 91, pp. 211–228, 2013.

[16] T. Meyers and B. Mather, "Empirical evaluation of GPS clock accuracy for isochronous droop-based inverters," in *Proc. IEEE Energy Convers. Congr. Expo.*, 2021, pp. 390–395.

[17] A. Bellini, S. Bifaretti, and F. Giannini, "A robust synchronization method for centralized microgrids," *IEEE Trans. Ind. Appl.*, vol. 51, no. 2, pp. 1602–1609, Mar./Apr. 2015.

[18] M. Litwin, D. Zielinski, and S. Stynski, "Remote synchronization of the microgrid to the utility grid without access to point of common coupling in the presence of disturbances," *IEEE Access*, vol. 10, pp. 27819–27831, 2022.

[19] M. S. Golsorkhi, M. Savaghebi, D. D.-C. Lu, J. M. Guerrero, and J. C. Vasquez, "A GPS-based control framework for accurate current sharing and power quality improvement in microgrids," *IEEE Trans. Power Electron.*, vol. 32, no. 7, pp. 5675–5687, Jul. 2017.

[20] M. S. Golsorkhi, D. D.-C. Lu, and J. M. Guerrero, "A GPS-based decentralized control method for islanded microgrids," *IEEE Trans. Power Electron.*, vol. 32, no. 2, pp. 1615–1625, Feb. 2017.

[21] H. Qian, Q. Xu, J. Zhao, and X. Yuan, "A robust GPS-based control scheme for power sharing and quality improvement in microgrid," *Int. J. Elect. Power Energy Syst.*, vol. 123, 2020, Art. no. 106324.

[22] H. Qian, Q. Xu, P. Du, Y. Xia, and J. Zhao, "Distributed control scheme for accurate power sharing and fixed frequency operation in islanded microgrids," *IEEE Trans. Ind. Electron.*, vol. 68, no. 12, pp. 12229–12238, Dec. 2021.

[23] H. Qian, Q. Xu, Y. Xia, J. Zhao, and P. Du, "Analysis and implementation of virtual impedance for fixed-frequency control strategy in microgrid," *IET Gener., Transmiss. Distrib.*, vol. 15, no. 15, pp. 2262–2276, 2021. [Online]. Available: https://ietresearch.onlinelibrary.wiley.com/doi/abs/10.1049/gtd2.12176
[24] S. Patel, S. Chakraborty, B. Lundstrom, S. M. Salapaka, and M. V. Salapaka, "Isochronous architecture-based voltage-active power droop for multi-inverter systems," *IEEE Trans. Smart Grid*, vol. 12, no. 2, pp. 1088–1103, Mar. 2021.
[25] L. S. Araujo, T. Caldognetto, D. I. Brandao, and P. Mattavelli, "Circulating harmonic current reduction in distorted voltage conditions using GPS-based synchronization," in *Proc. IEEE 13th Int. Symp. Power Electron. Distrib. Gener. Syst.*, 2022, pp. 1–6.
[26] Conseil international des grands réseaux électriques. Comité d'études C6 and International Council on Large Electric Systems, "Benchmark systems for network integration of renewable and distributed energy resources: Task force C6.04," (Brochures thématiques), CIGRÉ, 2014. [Online]. Available: https://books.google.it/books?id=v3PcoQEACAAJ
[27] *IRIG Standard 200-16 - IRIG Serial Time Code Formats*, Timing Committee Telecommunications and Timing Group, Range Commanders Council U. S. Army White Sands Missile Range, 2016.
[28] K. S. Yildirim, R. Carli, and L. Schenato, "Proportional-integral clock synchronization in wireless sensor networks," 2014, *arXiv:1410.8176*. [Online]. Available: https://arxiv.org/abs/1410.8176
[29] A. Monti, C. Muscas, and F. Ponci, *Phasor Measurement Units and Wide Area Monitoring Systems*, Amsterdam, The Netherlands: Elsevier Science, 2016.
[30] M. S. Padua, S. M. Deckmann, G. S. Sperandio, F. P. Marafao, and D. Colon, "Comparative analysis of synchronization algorithms based on PLL, RDFT and kalman filter," in *Proc. IEEE Int. Symp. Ind. Electron.*, 2007, pp. 964–970.

LUCAS SAVOI ARAUJO received the bachelor's degree in electrical engineering from the Federal University of Uberlandia, Uberlandia, Brazil, in 2013, the master's degree in electrical engineering from the University of Campinas (UNICAMP), Campinas, Brazil, in 2017, and the Ph.D. degree in electrical engineering from the Federal University of Minas Gerais (UFMG), Belo Horizonte, Brazil, in 2022. He was a Visiting Researcher with the University of Padova, Padua, Italy, in 2022. From 2017 to 2022, he was a Researcher with TESLA-Power Engineering group, Belo Horizonte, Brazil, working in industrial and government projects related to converter control for batteries, and real microgrid control, design, and implementation.

TOMMASO CALDOGNETTO (Senior Member, IEEE) received the M.S. (with Hons.) degree in electronic engineering and the Ph.D. degree in information engineering from the University of Padova, Padova, Italy, in 2012 and 2016, respectively. He is currently an Assistant Professor with the Department of Management and Engineering, University of Padova. His research interests include the control of grid-tied converters, microgrid architectures, converters for dc nanogrids, and real-time simulation for power electronics applications.

DANILO BRANDAO (Senior Member, IEEE) received the Ph.D. degree in electrical engineering from the University of Campinas, Campinas, Brazil, in 2015. He was a Visiting Scholar with the Colorado School of Mines, USA, in 2009 and 2013, a Visiting Scholar with the University of Padova, Padova, Italy, in 2014, and a Guest Professor with the Norwegian University of Science and Technology, Trondheim, Norway, in 2018 and 2020. He is currently an Assistant Professor with the Graduate Program in Electrical Engineering with the Federal University of Minas Gerais, Belo Horizonte, Brazil. His main research interests are control of grid-tied converters and microgrids. He is a Member of SOBRAEP.

PAOLO MATTAVELLI (Fellow, IEEE) received the M.S. (with Hons.) and Ph.D. degrees in electrical engineering from the University of Padova, Padova, Italy, in 1992 and 1995, respectively. He is a Full Professor with the University of Padova. His current Google scholar H-index is 80. His main research interests include analysis, modeling, and analog and digital control of power converters, grid-connected converters for renewable energy systems and microgrids, and high-temperature and high-power-density power electronics. He was an Associate Editor for the IEEE TRANSACTIONS ON POWER ELECTRONICSfrom 2003 to 2012. He is a Co-Editor-in-Chief for the IEEE TRANSACTIONS ON POWER ELECTRONICS. From 2005 to 2010, he was the Industrial Power Converter Committee Technical Review Chair for the IEEE TRANSACTIONS ON INDUSTRY APPLICATIONS. For terms 2003–2006, 2006–2009, and 2013–2015, he was a Member-at-large of the IEEE Power Electronics Society's Administrative Committee. He was the recipient of the Prize Paper Award in the IEEE TRANSACTIONS ON POWER ELECTRONICS in 2005, 2006, 2011, and 2012, and the 2nd Prize Paper Award at the IEEE Industry Applications Society Annual Meeting in 2007.

Open Access provided by 'Universitá degli Studi di Padova' within the CRUI CARE Agreement